ORIGINAL ARTICLE

Bonding of cast iron-aluminum in bimetallic castings by high-pressure die casting process

Mengwu Wu[1] · Jinpeng Yang[1] · Feng Huang[1] · Lin Hua[1] · Shoumei Xiong[2]

Abstract

A practical bimetallic casting consisting of aluminum matrix and cast iron inserts was manufactured via high-pressure die casting (HPDC) process. Different surface treatment methods for the cast iron inserts, including salt membrane plating and electrogalvanizing, were adopted to improve the bonding quality of bimetallic castings. Microstructure characterization on the bonding interface was conducted at different locations of bimetallic castings. Results indicate that compounds with flawless and continuously metallurgical bonding interface can be successfully fabricated by the HPDC process with the zinc rack plating treatment on the surface of cast iron inserts which results in a dense zinc coating with an average thickness of 8 μm. The melt flow speed and heat transition during solidification of the HPDC process are two key factors in determining the bonding integrity of bimetallic castings. With the dissolution and diffusion of the very thin zinc coating during solidification, there is no obvious aggregation of zinc element at the metallurgical bonding interface. Instead, a reaction layer with an irregular tongue-like morphology is formed with an average thickness of approximately 1 μm while it mainly consists of intermetallic phases $Al_{60}Cu_{30}Fe_{10}$, Fe_2Al_5, and Al_2FeSi.

1 Introduction

Bimetallic materials generally have superior comprehensive properties which are extremely difficult to achieve for single metal materials [1, 2]. Comparing to other bimetal bonding processes, the solid–liquid bimetal compound casting has been extensively used in modern industry with the advantages of good interfacial bonding quality, high production efficiency, and wide range of applicable alloys [3–6]. For instance, the most typical application of this process in automotive is the manufacturing of aluminum engine cylinder block with cast iron liners. Fe-Al bimetallic cylinder block has been a subject of investigation for more than 20 years due to its excellent performance on lightweight and thermal

conductivity comparing to the traditional cast iron cylinder block [7, 8].

The challenge of solid–liquid compound casting is the realization of a firmly bonding between two metal components. The characteristic of a real "compound cast" part is the formation of metallurgical bonding interfacial zones where the cast alloy's components diffuse into the solid material partly via the formation of solid solutions, and partly via the formation of reaction phases [9–14]. It has been proposed that an excellent metallurgical interface is of great importance to guarantee the physical and mechanical properties of bimetallic castings [15–18]. However, due to the difference in the thermal-physical properties, metallurgical bonding is extremely difficult to achieve for compound casting of dissimilar metals. Even for similar metallic couples, owing to the formation of oxide layer on surface of the solid substrate, the wettability between solid-state and liquid-state metals is largely impaired, leading to an incompatible and poor bonding between two metal components [19, 20]. There are a number of attempts to protect the surface of solid substrate metals from oxidation and to obtain an excellent metallurgical bonding between similar and also dissimilar metallic couples. Jiang et al. [21] found

✉ Mengwu Wu
  wumw@whut.edu.cn

1 Hubei Key Laboratory of Advanced Technology
  for Automotive Components, Wuhan University
  of Technology, Wuhan 430070, China

2 School of Materials Science and Engineering, Tsinghua
  University, Beijing 100084, China

Fig. 1 Configuration of the practical bimetallic casting and illustration of the locations of specimens extracted for microstructure characterization
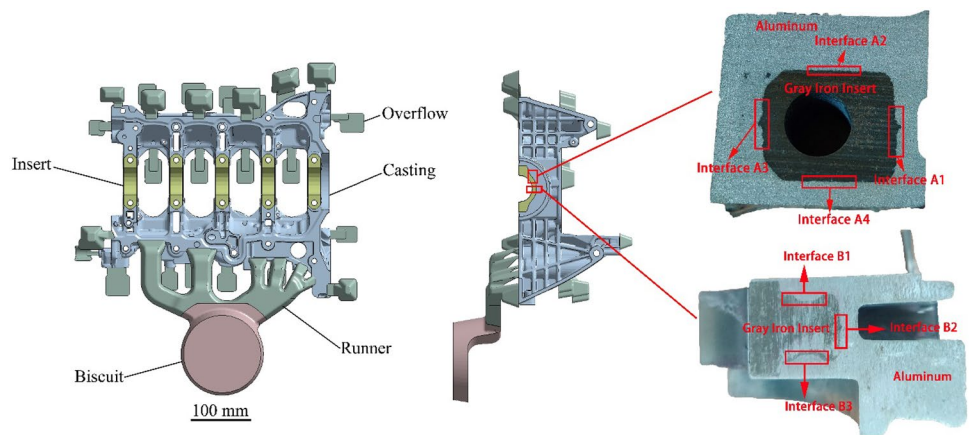
that a surface treatment method for steel inserts, i.e., a combination of coating surface modifier and aluminizing, could promote the formation of a metallurgical bonding interface between carbon steel and ZL114A aluminum alloy during compound casting process. Koerner et al. [22–24] pointed out that wrought Al-cast Al bimetallic castings with flawless metallic interface can be successfully produced by replacing the oxide layer on surface of wrought Al substrate with a zinc layer. Feng et al. [25] investigated the influence of coating materials on the overcast joining of aluminum alloys and concluded that Ni coating was superior over Cu coating. Ren et al. [26, 27] reported that Al–Mg bimetallic castings could be successfully fabricated by solid–liquid compound casting and they studied the effect of pouring temperature on the interfacial microstructure and mechanical properties of overcast joints.

According to literature review, most of the existing research works relating to the solid–liquid compound casting are based on the sand mold or permanent mold casting process. The HPDC process is the preferred choice for the mass production of light metal castings in the automotive, electronics, communications, and other fields [28–31]. Comparing to the sand mold and permanent mold casting processes, the much shorter heating and cooling times during the HPDC process represent a great challenge for the solid–liquid bimetal compound casting. Since the time is extremely inadequate for the diffusion and reaction between the two metal alloys during solidification of the HPDC process, it is difficult to achieve metallurgical bonding for bimetallic castings. Accordingly, the fabrication of bimetallic castings by using the HPDC process is still a relatively unexplored area, especially for the Fe-Al bimetallic castings

while there are large differences between the two types of metals relating to the thermal-physical properties, including the melting temperature.

In this study, a practical bimetallic casting consisting of aluminum matrix and cast iron inserts was manufactured by the HPDC process. Different surface treatment methods for the cast iron inserts were adopted to improve the bonding quality of bimetallic castings. Microstructure characterization on the bonding interface of bimetallic castings and simulation of the HPDC process were both conducted, based on which the effects of surface treatment methods and casting process on the bonding quality of bimetallic castings were investigated.

2 Experimental

2.1 Materials and surface treatment

A practical bimetallic casting named "bottom cylinder block" with complex structure was produced as shown in Fig. 1. For lightweight purpose, the component is mostly made of A380 aluminum alloy, while the part of bearing housing is made of HT250 gray cast iron to reduce friction between the crankshaft and bearing housing and also increase local strength. According to the analysis of inductive coupled plasma (ICP) and C-S analyzer, the chemical compositions of A380 aluminum alloy and HT250 gray cast iron are listed in Table 1 and Table 2, respectively.

In order to improve the bonding quality of bimetallic castings, different surface treatment methods were used for the gray iron inserts. The main purpose of surface treatment

Table 1 Chemical composition of the A380 aluminum alloy (wt%)

Si	Cu	Fe	Mn	Mg	Zn	Ni	Sn	Al
9.01	3.25	1.25	0.19	0.14	0.99	0.06	0.02	Bal

Table 2 Chemical composition of the HT250 gray cast iron (wt%)

C	Si	Mn	S	P	Fe
3.08	1.92	0.99	0.08	0.03	Bal

Table 3 Six groups of experiments distinguished by the surface treatment methods for gray iron inserts

Code	Surface treatment
1#	No treatment except for being cleaned
2#	Salt membrane plating
3#	Zinc barrel plating for 1 h
4#	Zinc barrel plating for 2 h
5#	Zinc barrel plating for 3 h
6#	Zinc rack plating for 1 h

is to protect the solid metal surface from oxidation and to enhance the wettability of aluminum melt on its surface. The surface treatment methods used in this study include salt membrane plating and electrogalvanizing. Firstly, the surface of the gray iron inserts was sandblasted to remove oxides, and then rinsed using a 0.5 mol/L hydrochloric acid and an ethanol, respectively. After being cleaned, the gray iron inserts were immersed into a solution of sodium chloride and ammonium chloride with a weight ratio of 1:1 and a total concentration of 100 g/L at 50 °C for 15 min. Afterward, the gray iron inserts were taken out and dried. Another surface treatment method after the gray iron inserts being cleaned was electrogalvanizing with an electrolyte containing 150 g/L $ZnSO_4$, 50 g/L $N_2H_8SO_4$, and 15 g/L boric acid. Different thicknesses of zinc coating were expected to obtained by the barrel plating and rack plating processes. With the same current density of 30 mA/cm^2 at room temperature, the time for barrel plating was 1 h, 2 h, and 3 h, respectively, while the time for rack plating was 1 h. Consequently, six groups of experiments were constructed in this study according to different surface treatment methods for gray iron inserts as shown in Table 3.

2.2 Casting process

Once the surface treatment process was completed, the gray iron inserts were heated to 200 °C by means of electromagnetic induction and then rapidly placed inside the die casting mold for pouring. A UB1650iV cold chamber die casting unit was used for the fabrication of bimetallic castings. In order to balance the requirements of a sound metallic bonding and a good overall quality of the bimetallic castings, key process parameters used during the HPDC process were set as pouring temperature of the aluminum melt (650 °C), initial mold temperature (200 °C), and intensification casting

pressure (80 MPa). With a diameter of 130 mm, the plunger was first moving in a speed constantly accelerated from 0 to 0.3 m/s for 522 mm at the slow shot stage. Then the plunger speed was rapidly accelerated to 3.4 m/s and the HPDC process stepped into the fast shot stage. Intensification casting pressure was applied when the plunger was moving to 750 mm and maintained until the casting solidified.

2.3 Microstructure characterization

To investigate the bonding quality and interfacial microstructure of the bimetallic castings, metallographic specimens were cut from the bimetallic castings as illustrated in Fig. 1. Since there were five gray iron inserts in the bimetallic castings, the rightmost one was chosen to analyze the bonding quality with the aluminum matrix. Due to the complex structure of both the gray iron insert and aluminum matrix, seven bonding interfaces marked "A1," "A2," "A3," and "A4" and "B1," "B2," and "B3" from two sections were selected for comparative study. A ZEISS scope A1 optical microscope (OM), a JSM-IT300 scanning electron microscope (SEM) equipped with energy-dispersive spectrometer (EDS), and a FEI Talos F200X transmission electron microscope (TEM) were used for metallography observation. The metallographic specimens were treated following the standard metallographic procedures and etch was not required.

2.4 Simulation of the HPDC process

The Anycasting software was used to analyze the filling and solidification sequence of the aluminum melt during the HPDC process. Thermo-physical parameters of the relevant materials, such as the two metal alloys and die casting mold, were determined according to the material database of the software itself. Table 4 shows the main thermo-physical parameters of A380 aluminum alloy and HT250 gray cast iron used in the simulation. The process parameters of the HPDC process were set in accordance with those of the die casting experiment as mentioned in Sect. 2.2. The non-uniform meshing technique was adopted to improve the simulation efficiency and also accuracy, while fine meshes were utilized for the bimetallic bonding interface region with a mesh size of 0.5 mm. Virtual sensors were set at the concerned locations to record the melt flow speed and temperature data within the whole filling and solidification process.

Table 4 Main thermo-physical parameters of A380 aluminum alloy and HT250 gray cast iron

Alloy	Density (kg/m^3)	Specific heat (J/(kg•K))	Thermal conductivity (W/(m•K))	Liquidus temperature (°C)	Solidus temperature (°C)	Latent heat (J/kg)
A380	2740	963	96	590	535	389,000
HT250	7150	544	58	1228	1148	200,000

Fig. 2 Appearance of the gray iron inserts: (**a**) no treatment except for being cleaned, (**b**) salt membrane plating, and (**c**) electrogalvanizing
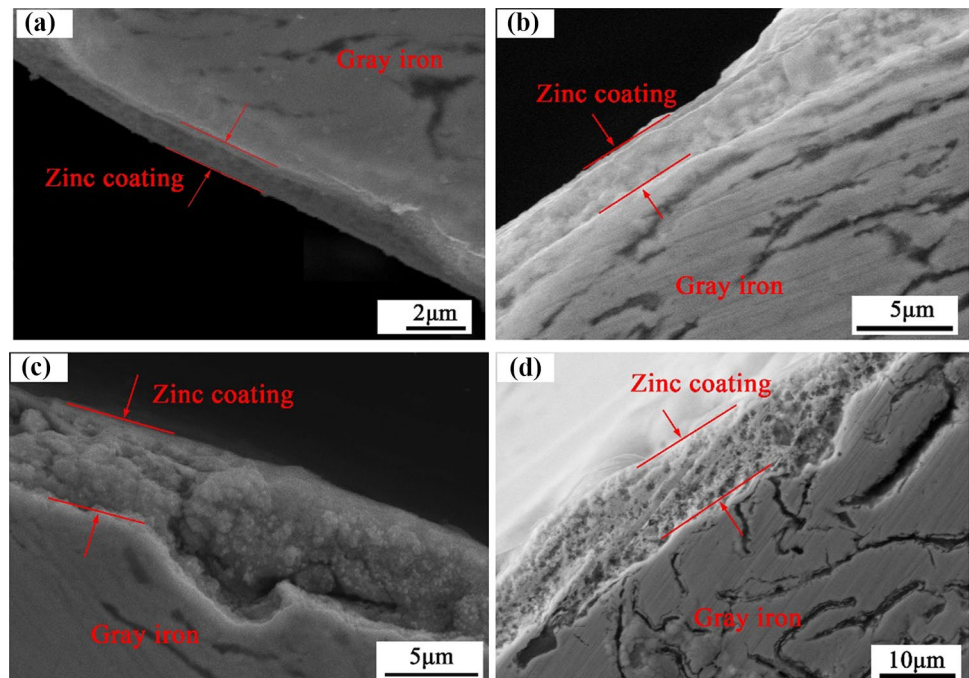

3 Results

3.1 Surface morphology of the gray iron inserts

Figure 2 shows the surface macro-morphology of gray iron inserts with different surface treatment methods. By sandblasting and cleaning, the surface of the gray iron insert in Fig. 2a reveals its natural color. An obvious salt membrane is formed on the surface of the gray iron insert as shown in Fig. 2b. It has been reported that the use of a sodium chloride solution or ammonium chloride solution is favorable to the removal of oxide layer generated at the surface of gray iron inserts by chemical reaction [21]. Meanwhile, the salt membrane acts as a barrier to prevent the gray iron inserts from further oxidation, thereby enhancing the wettability between the gray iron inserts and aluminum melt. By the surface treatment method of electrogalvanizing, either through barrel plating or rack plating process, the surface of the gray iron insert in Fig. 2c exhibits a metallic luster of zinc. It has been proved that zinc is well suited as a coating material for the solid–liquid bimetal compound casting [22, 23]. The oxidation of zinc will result in the formation of a

thin but dense zinc oxide film, which can effectively prevent the inner zinc metal and gray iron inserts from oxidation. During the solid–liquid compound casting process, the thin zinc oxide film will fall off from the gray iron inserts due to the scouring effect of the melt, letting the fresh zinc or gray iron to be exposed to the aluminum melt. Other significant advantages of zinc include a relative low melting temperature of 420 °C and a high solubility in aluminum at elevated temperature. These crucial properties are beneficial to the diffusion and chemical reaction between the gray iron inserts and molten aluminum alloy.

It is known that the quality of zinc coating formed by electrogalvanizing is deeply related to the specific electroplating process and the corresponding process parameters. Figure 3 shows the cross-section morphology of zinc coating on surface of gray iron inserts with different electrogalvanizing processes. It can be seen from Fig. 3a–c that with the increase of the time for barrel plating from 1 h to 2 and 3 h, the average thickness of the zinc coating increases from 1 to 2.5 and 4.5 µm. For rack plating with 1 h, the average thickness of the zinc coating increases to 8 µm as shown in Fig. 3d. Figure 4 indicates the surface micro-morphology of the gray iron inserts with different electrogalvanizing processes.

Fig. 3 Cross-section morphology of the gray iron inserts and thickness of zinc coating: (**a**) zinc barrel plating for 1 h, (**b**) zinc barrel plating for 2 h, (**c**) zinc barrel plating for 3 h, and (**d**) zinc rack plating for 1 h

In combination with the corresponding EDS mapping results, it can be concluded that for zinc coating, the variation trend of coating density is consistent with the thickness mentioned above. With barrel plating for 1 h, the surface of the zinc coating is very uneven as noted in Fig. 4a. A sparse zinc coating leads to a large number of iron atoms to be exposed to the surface (Fig. 4b, c).

This situation is substantially improved by increasing the time for barrel plating from 1 h to 2 and 3 h. For rack plating with 1 h, a dense zinc coating is obtained as shown in Fig. 4j–l, which is considered beneficial for protecting the gray iron inserts from oxidation and enhancing the wettability between the gray iron inserts and aluminum melt.
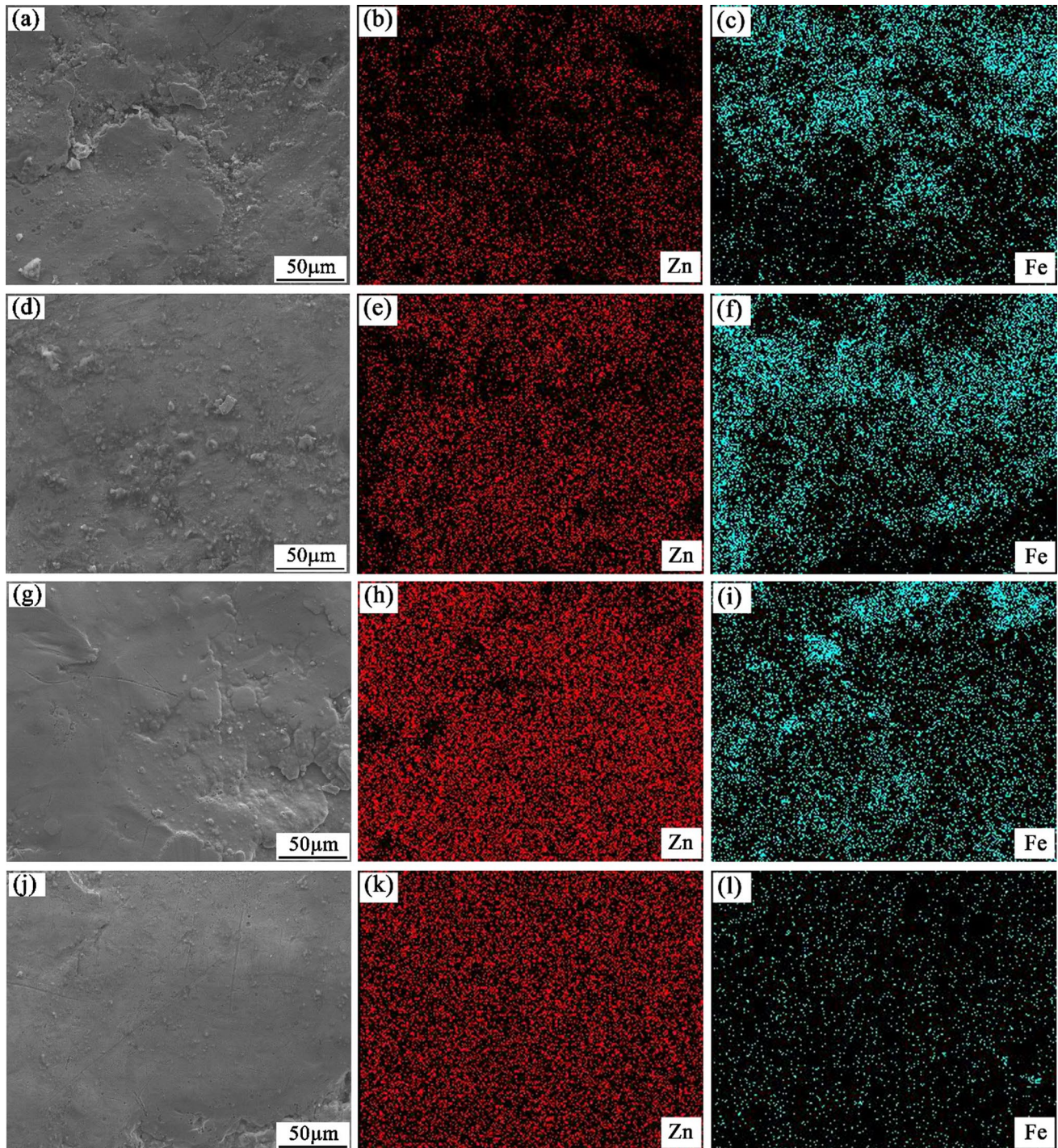

Fig. 4 Surface micro-morphology of the gray iron inserts and the corresponding EDS mapping results: (**a–c**) zinc barrel plating for 1 h, (**d–f**) zinc barrel plating for 2 h, (**g–i**) zinc barrel plating for 3 h, and (**j–l**) zinc rack plating for 1 h

3.2 Bonding quality of the bimetallic castings

Microstructure characterization on the bonding interfaces was conducted to investigate the effect of surface treatment methods for the cast iron inserts on the bonding quality of bimetallic castings. Corresponding to the six experimental groups listed in Table 3, Fig. 5 shows the interfacial microstructure at the bonding interface A4 of bimetallic castings with different surface treatment methods for the gray iron inserts. A large gap with a width more than 20 μm is observed in the interfacial microstructure of bimetallic casting with no treatment except for being cleaned of the gray iron inserts as shown in Fig. 5a, leading to an incompatible and poor bonding between two metal components. By salt membrane plating of the gray iron inserts, the gap between the two metal components becomes narrow as illustrated in Fig. 5b. However, a large number of inclusions, perhaps salt membrane residues, are observed in the interfacial microstructure, resulting in a poor integrity of

the bimetallic castings. With zinc barrel plating of the gray iron inserts, the bonding quality of bimetallic castings is improved. Particularly, the gap width between the two metal components continues to decrease with the increase of the time for zinc barrel plating from 1 h to 2 and 3 h as noted in Fig. 5c–e. In the case of zinc rack plating for 1 h, the integrity of the compound interface of bimetallic castings is greatly increased. With the disappearance of the gap, a reaction layer forms between the two metal components as shown in Fig. 5f, which indicates that compounds with flawless and continuously metallurgical bonding interface are successfully fabricated.

To reveal the detailed characteristics of the reaction layer between the two metal components in Fig. 5f, high-magnification interfacial microstructure is observed by SEM as shown in Fig. 6. The reaction layer exhibits an irregular tongue-like morphology with an average thickness of approximately 1 μm. According to the EDS line scanning results, the distribution of the elements Al and Fe conforms to the Fick's law of diffusion [32]; i.e., the

Fig. 5 OM images of the microstructure at the bonding interface "A4"of bimetallic castings with different surface treatment methods for the gray iron inserts: (a) no treatment except for being cleaned, (b) salt membrane plating, (c) zinc barrel plating for 1 h, (d) zinc barrel plating for 2 h, (e) zinc barrel plating for 3 h, and (f) zinc rack plating for 1 h
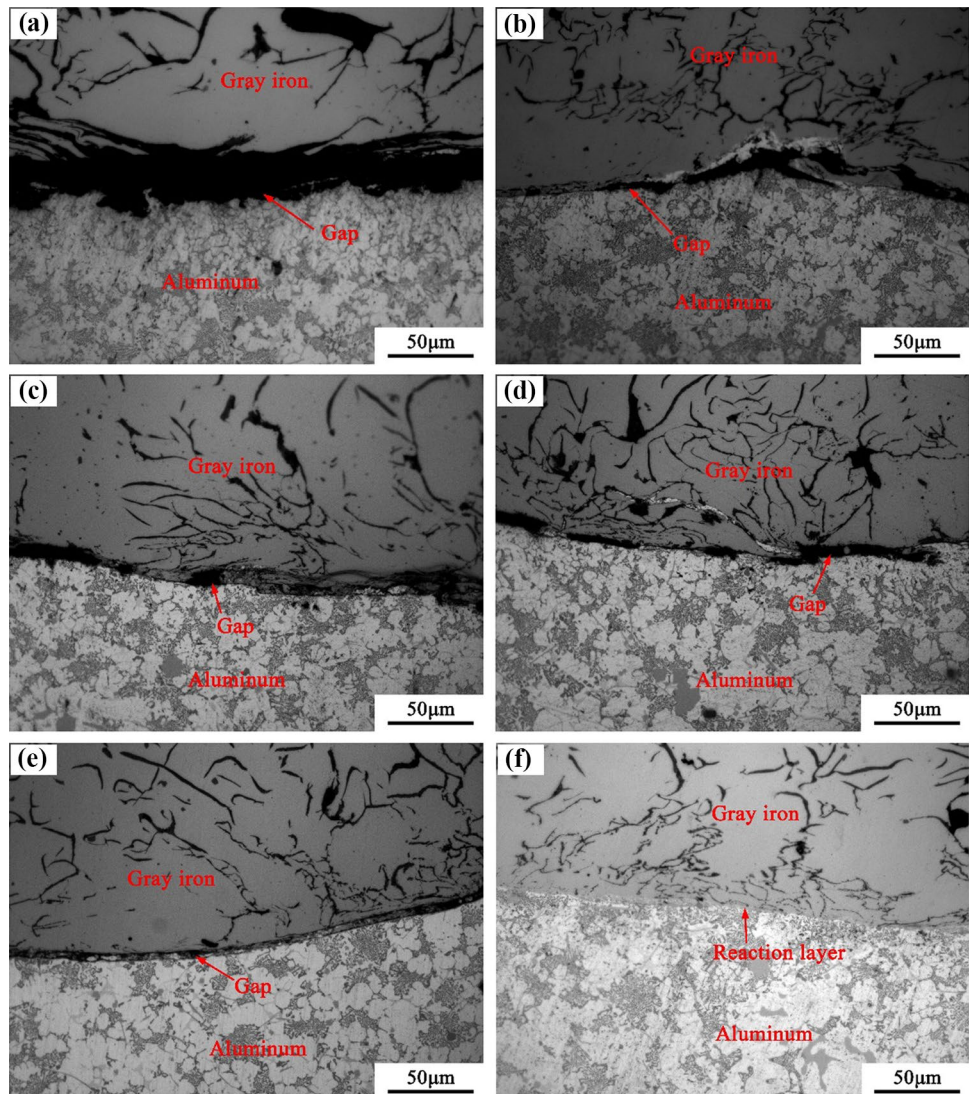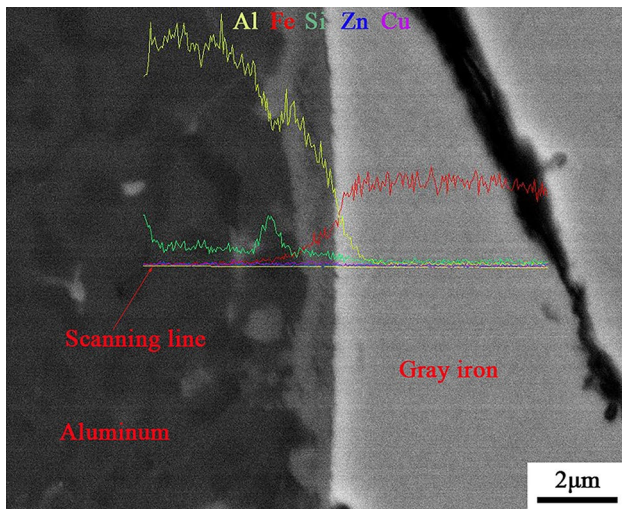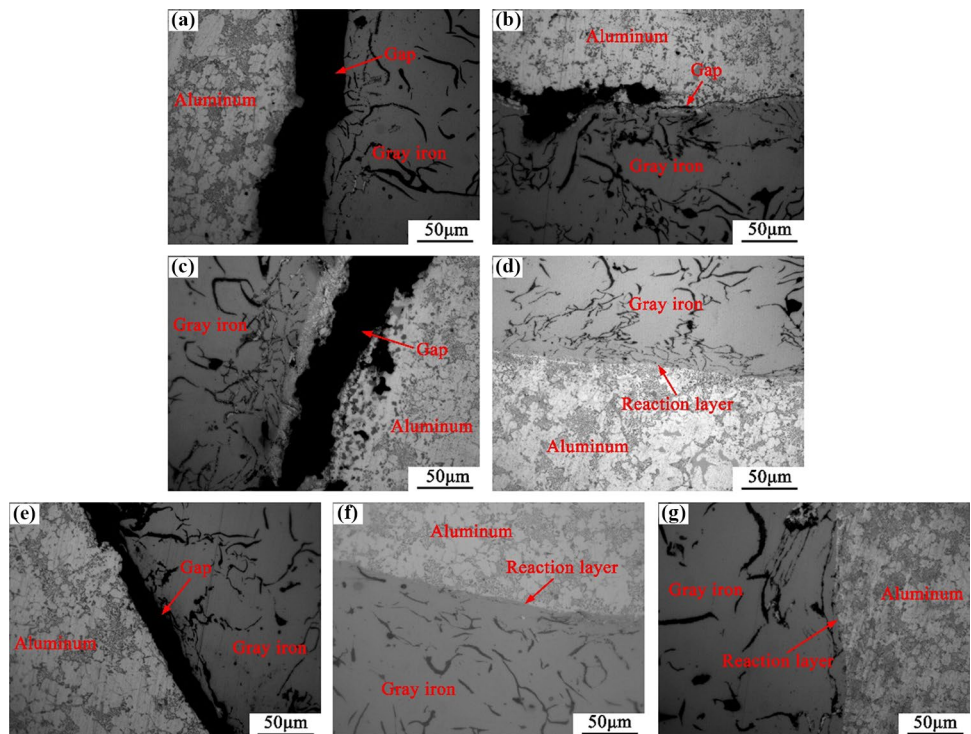
Fig. 6 High-magnification SEM image of the interfacial microstructure as shown in Fig. 5f and the corresponding EDS line scanning results

contents of Al and Fe decrease gradually along the thickness of the reaction layer, respectively, in the directions from the aluminum matrix to the gray iron insert and the opposite one. This phenomenon proves that diffusion and reaction between the two metal alloys undoubtedly happen during solidification of the compound casting process, which are essential and important conditions to guarantee a metallurgical bonding of the bimetallic castings.

Since the bimetallic casting in this study is a practical product with complex structure of both the gray iron insert and aluminum matrix, the bonding quality may vary greatly at different joint locations. Figure 7 illustrates the microstructure at different bonding interfaces of the bimetallic casting with a treatment of zinc rack plating for 1 h on surface of the gray iron inserts. It can be seen from Fig. 7a–d that among the four bonding interfaces in section A, only the bonding interface A4 conforms to the characteristics of metallurgical bonding, while large gaps appear in the microstructure at the bonding interfaces A1 and A3. For section B as shown in Fig. 7e–g, the reaction layer is observed both at the bonding interfaces B2 and B3. In particular, the bonding interface B2 is flawless with continuously metallurgical bonding, which is the ideal state to expect for bimetallic castings with superior comprehensive properties. As for the reason for the difference of the bonding quality between these bonding interfaces, this will be discussed in detail in the following section.

3.3 Phase distribution in the interfacial layer

To investigate the diffusion and reaction behavior between the two metal alloys during solidification of the compound casting process, element and phase distribution in the interfacial layer with metallurgical bonding was extracted by TEM and EDS as shown in Fig. 8 and Table 5. The TEM bright-field image (Fig. 8a) is clearly divided into three parts

Fig. 7 OM images of the microstructure at different bonding interfaces of the bimetallic casting with a treatment of zinc rack plating for 1 h on surface of the gray iron inserts: (**a**) A1, (**b**) A2, (**c**) A3, (**d**) A4, (**e**) B1, (**f**) B2, and (**g**) B3

by the reaction layer with an irregular tongue-like morphology. They are the A380 aluminum alloy matrix, the reaction layer, and HT250 gray iron insert from top to bottom. It can be seen from Fig. 8c–f and Table 5 that except for elements Al and Fe, there also exists the diffusion and reaction of Cu and Si in the reaction layer. Here, the reaction layer is just the so-called intermetallic compound (IMC) layer where the elements mentioned above exist in the form of intermetallic compound. Most of the elements Al and Si come from the

A380 aluminum alloy matrix by diffusion. Different from the element Si in the microstructure of A380 aluminum alloy in the form of primary or eutectic Si phase, it is in the form of intermetallic compound, resulting in a uniform distribution in the reaction layer on a micron level. Due to a high melting point of the HT250 gray iron, the diffusion of the element Fe is extremely difficult which leads to a relative low content in the reaction layer. It is noteworthy that the element Cu unexpectedly accumulates in the reaction layer. According

Fig. 8 Element distribution and phase identification in the interfacial layer with metallurgical bonding: (**a**) TEM bright-field image showing interfacial microstructure, (**b**) microbeam electron diffraction pattern of point 3, and (**c**–**f**) the corresponding EDS mapping results
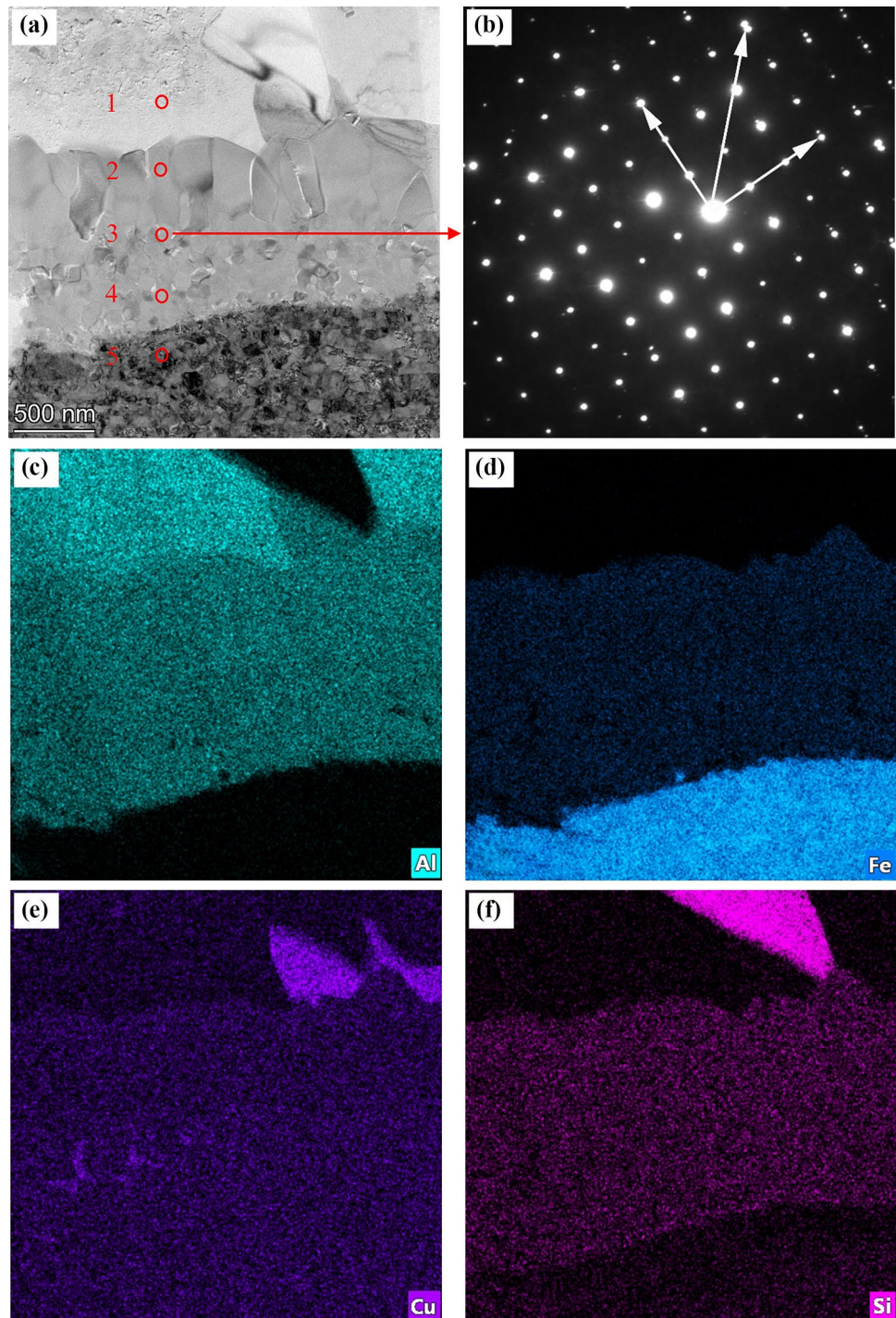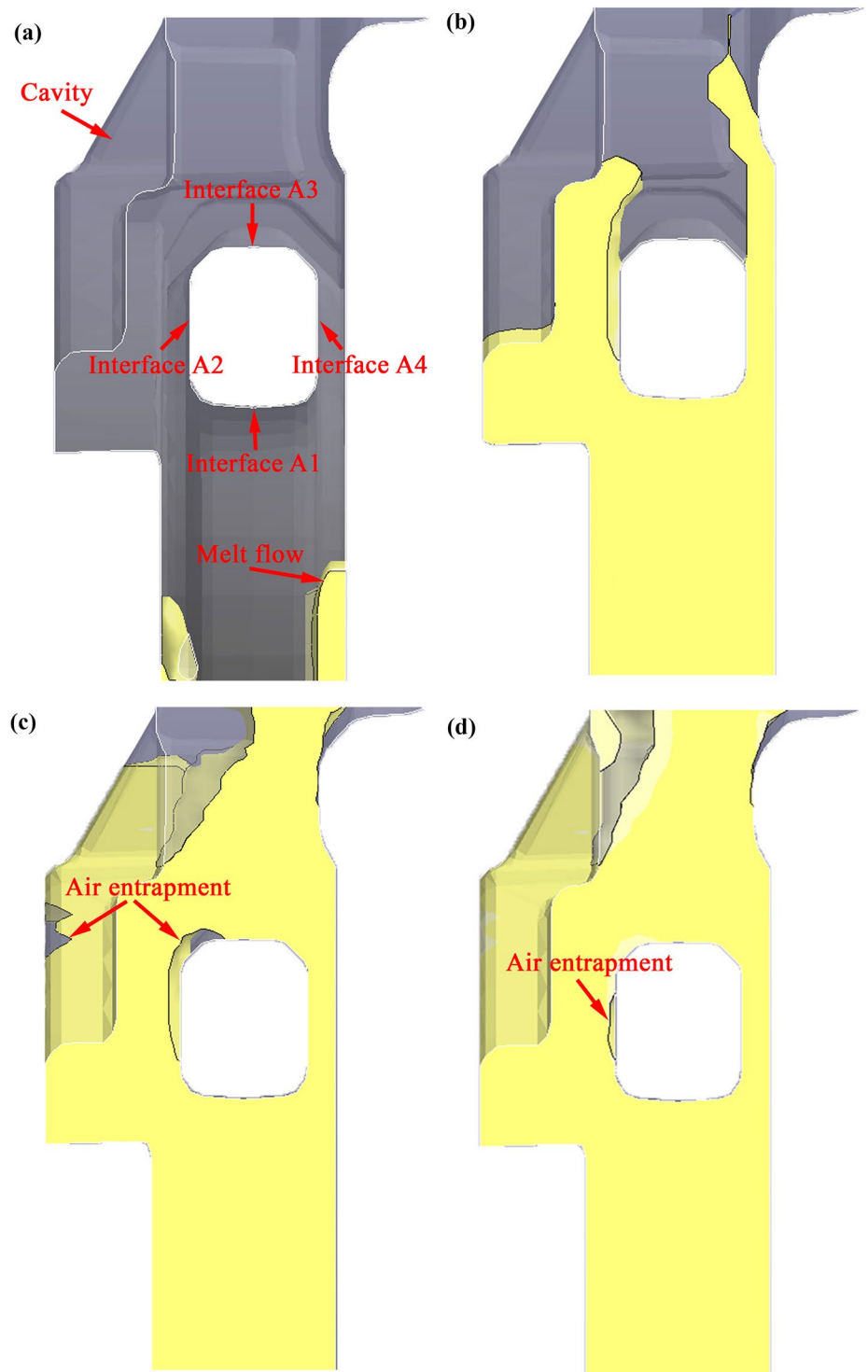
Table 5 EDS analysis results corresponding to the points indicated in Fig. 8a

Number	Element compositions (at%)						
	Al	Fe	Cu	Si	C	Mn	Zn
Point 1	79.8	0.09	16.97	1.74	0.23	0.04	0.98
Point 2	53.15	12.88	21.51	9.18	1.62	1.22	0.34
Point 3	58.06	10.66	21.07	7.3	1.48	0.65	0.44
Point 4	20.98	48.31	18.89	6.4	3.64	0.42	1.25
Point 5	1.14	74.1	16.11	3.61	4.17	0.67	0.04

Fig. 9 Simulated results of mold filling near section A during the HPDC process at different times: (**a**) 0.3199 s, (**b**) 0.3233 s, (**c**) 0.3287 s, and (**d**) 0.3302 s

546 The International Journal of Advanced Manufacturing Technology (2022) 120:537–549

to the EDS analysis in Table 5, the content of Cu in the reaction layer is even higher than that of the A380 aluminum alloy matrix where it comes from by diffusion. This may be because the radius of the Cu atom is much closer to that of the Fe atom comparing to the radius of the Al atom, which facilitates the diffusion of Cu atoms from A380 aluminum alloy matrix towards the reaction layer [33]. Another phenomenon is also retrieved from Fig. 8 and Table 5 that there is no obvious aggregation of the element Zn in the interfacial layer with metallurgical bonding.

Figure 8b shows the electron diffraction pattern of point 3 marked in Fig. 8a. In combination with the EDS analysis in Table 5, the phase at point 3 is identified to be $Al_{60}Cu_{30}Fe_{10}$. In fact, the phase distribution in the interfacial layer is extremely complex due to the reaction of the multiple elements with each other, which leads to the formation of multiple intermetallic compounds. Other phases in the reaction layer may include Fe_2Al_5 and Al_2FeSi [7, 21]. The formation of intermetallic phases is related to the mixing enthalpy between different elements, while the lower the mixing enthalpy, the more likely the corresponding intermetallic phase will form accompanied with the release of latent heat.

4 Discussion

It is well known that the metallurgical bonding of bimetallic castings is guaranteed by the formation of a diffusion and reaction zone between the two metallic materials. Due to the large difference of the thermal-physical properties between Fe and Al, as well as the oxide film formed at the surface of solid inserts, it is difficult to achieve metallurgical bonding for Fe-Al bimetallic castings. Furthermore, the challenge is significantly increased with the adoption of the HPDC process in the solid–liquid bimetal compound casting. In this aspect, the present work is meaningful while cast iron-aluminum compounds with flawless and continuously metallurgical bonding interface are successfully fabricated by the HPDC process with a zinc rack plating treatment on the surface of cast iron inserts. However, for the practical bimetallic casting in this study with complex structure of both the gray iron insert and aluminum matrix, not all bonding interfaces achieve metallurgical bonding as indicated in Fig. 7. The cause of this phenomenon may be ascribed to the difference in solidification conditions at these interfaces. Except for a sufficient thick and dense zinc coating to protect the gray iron inserts from oxidation, appropriate thermodynamic conditions of the aluminum melt are also required for the metallurgical bonding between the two metallic materials.

Figure 9 shows the simulated results of mold filling near section A at different times. It can be seen that the interfaces A1 and A3 are perpendicular to the melt flow direction. Due

to the influence of the cavity structure, the melt flow direction dramatically changes near the interface A2, resulting in air entrapment in the aluminum melt as shown in Fig. 9c, d. Comparatively, the melt flow near the interface A4 is the most ideal with a flow direction parallel to the interface. Figure 10 shows the simulated quantitative results of the melt flow speed and temperature at different interfaces. It can be noted from Fig. 10a that the melt flow speed at interface A4 is much higher than that at interfaces A1, A2, and A3. Since only the interface A4 conforms to the characteristics of metallurgical bonding as shown in Fig. 7a–d, it can be concluded that a high melt flow speed is beneficial to the formation of metallurgical bonding interface between the two metallic materials. Combining the metallographic results as indicated in Fig. 7e–g and the simulated results as shown in Fig. 10b, a similar conclusion also can be made that the flawless and continuously metallurgical bonding of
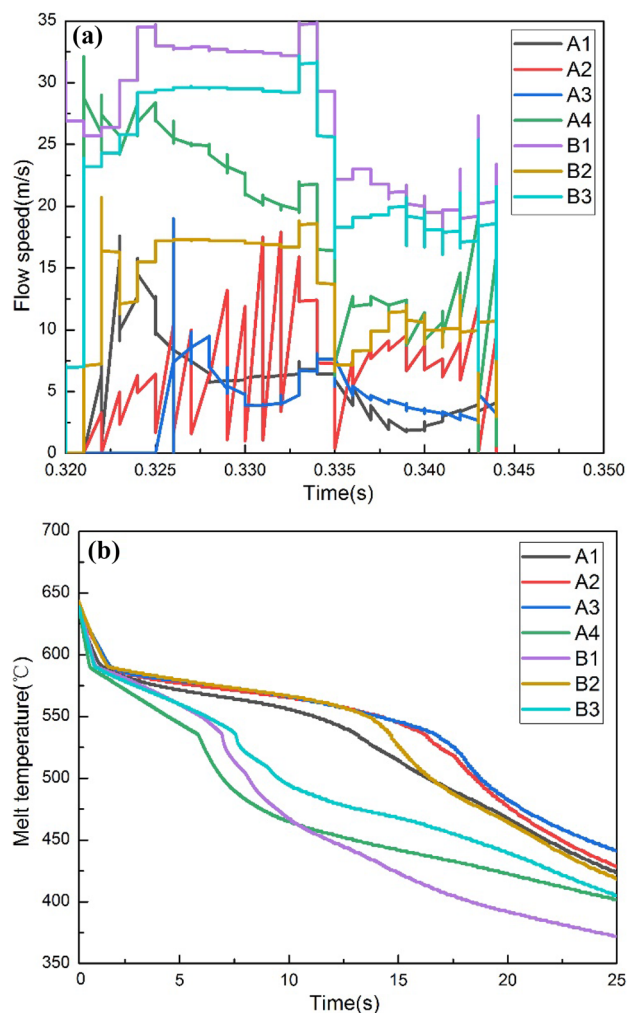

Fig. 10 Simulated results of the melt flow speed and temperature at different interfaces: (**a**) melt flow speed and (**b**) melt temperature (Note that for each interface, the simulated data is exacted from the center point to represent the whole interface.)

② Springer

Fig. 11 SEM images of the interfacial microstructure and the corresponding EDS mapping results of the zinc element: (**a** and **b**) interface with metallurgical bonding and (**c** and **d**) interface without metallurgical bonding
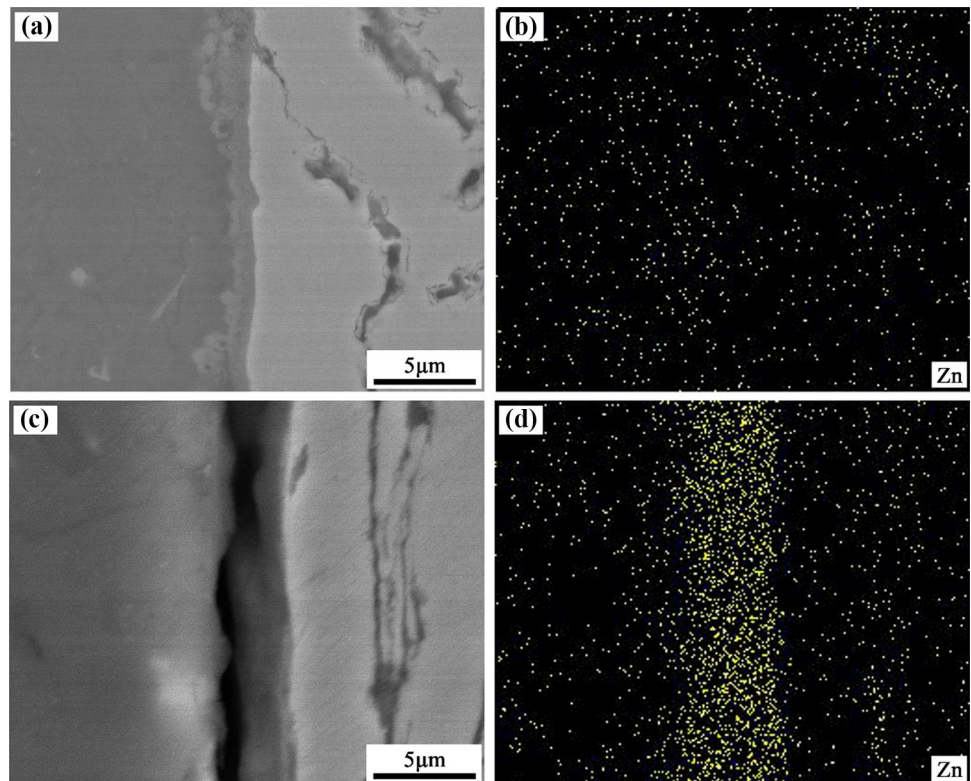
interface B2 is due to a much lower cooling rate and slower drop of the temperature of the aluminum melt comparing to those at interfaces B1 and B3.

According to the analysis mentioned above, the melt flow speed and heat transition during solidification of the HPDC process are two key factors in determining the bonding integrity of bimetallic castings. With a high flow speed and temperature of the aluminum melt, a large amount of thermal shock acts upon the gray iron inserts, resulting in the dissolution and diffusion of the zinc coating. This can be additionally elucidated in Fig. 11. No obvious aggregation of the element Zn is detected in the interfacial layer with metallurgical bonding, but a considerable amount of it remains at the interface without metallurgical bonding. With the sufficient dissolution and diffusion of the zinc coating, the fresh and clean surface of gray iron inserts is exposed, which is beneficial to the diffusion and reaction between the two metallic materials. Meanwhile, studies have shown that a too thick zinc coating is not conducive to a firmly metallurgical bonding of bimetallic castings [22].

5 Conclusions

In this study, the effects of surface treatment methods for the gray iron inserts and casting process on the bonding quality of a practical bimetallic casting have been investigated. The following conclusions can be drawn:

1. With the rack plating process for 1 h, a dense zinc coating is formed on surface of the gray iron inserts with an average thickness of 8 μm.
2. Cast iron-aluminum compounds with flawless and continuously metallurgical bonding interface can be successfully fabricated by the HPDC process with the zinc rack plating treatment on the surface of cast iron inserts.
3. The melt flow speed and heat transition during solidification of the HPDC process are two key factors in determining the bonding integrity of bimetallic castings. With the dissolution and diffusion of the very thin zinc coating during solidification, there is no obvious aggregation of zinc element at the metallurgical bonding interface, while the content of Cu is higher than that of the A380 aluminum alloy matrix where it comes from by diffusion.
4. In the interfacial microstructure of bimetallic castings with metallurgical bonding, a reaction layer with an irregular tongue-like morphology is formed with an average thickness of approximately 1 μm consisting of intermetallic phases $Al_{60}Cu_{30}Fe_{10}$, Fe_2Al_5, and Al_2FeSi.

Data availability The data sets supporting the results of this article are presented within the article itself.

Declarations

Ethics approval Not applicable.

Consent to participate The authors have informed consent.

Consent for publication Not applicable.

Conflict of interest The authors declare no competing interests.

References

1. Jin K, Yuan QW, Tao J, Domblesky J, Guo XZ (2019) Analysis of the forming characteristics for Cu/Al bimetal tubes produced by the spinning process. Int J Adv Manuf Technol 101(1–4):147–155. https://doi.org/10.1007/s00170-018-2836-6

2. Shen YY, Jia Q, Zhang X, Liu RH, Wang YM, Cui YY, Yang R (2021) Tensile behavior of SiC fiber-reinforced gamma-TiAl composites prepared by suction casting. Acta Metall Sin (Engl Lett) 34(7):932–942. https://doi.org/10.1007/s40195-020-01170-5

3. Hu Q, Jiang ZL, Jiang WM, Li GY, Guan F, Jiang HX, Fan ZT (2019) Interface characteristics of Mg/Al bimetal produced by a novel liquid-liquid compound casting process with an Al interlayer. Int J Adv Manuf Technol 101(5–8):1125–1132. https://doi.org/10.1007/s00170-018-2990-x

4. Liu T, Wang QD, Sui YD, Wang QG, Ding WJ (2016) An investigation into interface formation and mechanical properties of aluminum-copper bimetal by squeeze casting. Mater Des 89:1137–1146. https://doi.org/10.1016/j.matdes.2015.10.072

5. Liu GP, Wang QD, Liu T, Ye B, Jiang HY, Ding WJ (2017) Effect of T6 heat treatment on microstructure and mechanical property of 6101/A356 bimetal fabricated by squeeze casting. Mater Sci Eng A 696:208–215. https://doi.org/10.1016/j.msea.2017.04.072

6. Ding ZY, Zhang NF, Yu L, Lu WQ, Li JG, Hu QD (2021) Recent progress in metallurgical bonding mechanisms at the liquid/solid interface of dissimilar metals investigated via in situ X-ray imaging technologies. Acta Metall Sin (Engl Lett) 34(2):145–168. https://doi.org/10.1007/s40195-021-01193-6

7. Jiang WM, Fan ZT, Li GY, Liu XW, Liu FC (2016) Effects of hot-dip galvanizing and aluminizing on interfacial microstructures and mechanical properties of aluminum/iron bimetallic composites. J Alloy Compd 688:742–751. https://doi.org/10.1016/j.jallcom.2016.07.085

8. Springer H, Kostka A, Payton EJ, Raabe D, Kaysser-Pyzalla A, Eggeler G (2011) On the formation and growth of intermetallic phases during interdiffusion between low-carbon steel and aluminum alloys. Acta Mater 59(4):1586–1600. https://doi.org/10.1016/j.actamat.2010.11.023

9. Liu T, Wang QD, Sui YD, Wang QG (2016) Microstructure and mechanical properties of overcast 6101–6101 wrought Al alloy joint by squeeze casting. J Mater Sci Technol 32(4):298–304. https://doi.org/10.1016/j.jmst.2015.11.020

10. Li GY, Jiang WM, Guan F, Zhu JW, Zhang Z, Fan ZT (2021) Microstructure, mechanical properties and corrosion resistance of A356 aluminum/AZ91D magnesium bimetal prepared by a compound casting combined with a novel Ni-Cu composite interlayer. J Mater Process Technol 288:116874. https://doi.org/10.1016/j.jmatprotec.2020.116874

11. Xu JZ, Gao XJ, Jiang ZY, Wei DB, Jiao SH (2016) Microstructure and hot deformation behaviour of high-carbon steel/ low-carbon steel bimetal prepared by centrifugal composite casting. Int J Adv Manuf Technol 86(1–4):817–827. https://doi.org/10.1007/s00170-015-8232-6

12. Zhu ZA, Shi RH, Klarner AD, Luo AA, Chen YQ (2020) Predicting and controlling interfacial microstructure of magnesium/ aluminum bimetallic structures for improved interfacial bonding. J Magnes Alloy 8(3):578–586. https://doi.org/10.1016/j.jma.2020.03.004

13. He K, Zhao JH, Li P, He JS, Tang Q (2016) Investigation on microstructures and properties of arc-sprayed-Al/AZ91D bimetallic material by solid-liquid compound casting. Mater Des 112:553–564. https://doi.org/10.1016/j.matdes.2016.09.085

14. Zhang H, Chen YQ, Luo AA (2014) A novel aluminum surface treatment for improved bonding in magnesium/aluminum bimetallic castings. Scr Mater 86:52–55. https://doi.org/10.1016/j.scriptamat.2014.05.007

15. Zare GR, Divandari M, Arabi H (2013) Investigation on interface of Al/Cu couples in compound casting. Mater Sci Technol 29(2):190–196. https://doi.org/10.1179/1743284712Y.0000000096

16. Li GY, Jiang WM, Yang WC, Jiang ZL, Guan F, Jiang HX, Fan ZT (2019) New insights into the characterization and formation of the interface of A356/AZ91D bimetallic composites fabricated by compound casting. Metall Mater Trans A 50(2):1076–1090. https://doi.org/10.1007/s11661-018-5022-4

17. Babaee MH, Maleki A, Niroumand B (2019) A novel method to improve interfacial bonding of compound squeeze cast Al/ Al-Cu macrocomposite bimetals: simulation and experimental studies. Trans Nonferrous Met Soc China 29(6):1184–1199. https://doi.org/10.1016/S1003-6326(16)64261-9

18. Hajjari E, Divandari M, Razavi SH, Emami SM, Homma T, Kamado S (2011) Dissimilar joining of Al/Mg light metals by compound casting process. J Mater Sci 46(20):6491–6499. https://doi.org/10.1007/s10853-011-5595-4

19. Schwankl M, Himmler D, Urban M, Koerner C (2018) Optimization of mechanical properties of Al-Al-compound castings by adapted heat treatment. Adv Eng Mater 20(12):1800400. https://doi.org/10.1002/adem.201800400

20. Schwankl M, Wedler J, Koerner C (2016) Wrought Al-cast Al compound casting based on zincate treatment for aluminum wrought alloy inserts. J Mater Process Technol 238:160–168. https://doi.org/10.1016/j.jmatprotec.2016.07.001

21. Jiang WM, Fan ZT, Li C (2015) Improved steel/aluminum bonding in bimetallic castings by a compound casting process. J Mater Process Technol 226:25–31. https://doi.org/10.1016/j.jmatprotec.2015.06.032

22. Koerner C, Schwankl M, Himmler D (2014) Aluminum–aluminum compound castings by electroless deposited zinc layers. J Mater Process Technol 214:1094–1101. https://doi.org/10.1016/j.jmatprotec.2013.12.014

23. Rubner M, Gunzl M, Koerner C, Singer RF (2011) Aluminium–aluminium compound fabrication by high pressure die casting. Mater Sci Eng A 528(22–23):7024–7029. https://doi.org/10.1016/j.msea.2011.05.076

24. Papis KJM, Hallstedt B, Loeffler JF, Uggowitzer PJ (2008) Interface formation in aluminium-aluminium compound casting. Acta Mater 56(13):3036–3043. https://doi.org/10.1016/j.actamat.2008.02.042

25. Feng J, Ye B, Zuo LJ, Wang QD, Wang QG, Jiang HY (2017) Bonding of aluminum alloys in compound casting. Metall Mater Trans A 48(10):4632–4644. https://doi.org/10.1007/s11661-017-4252-1

26. Ren QS, Zhao CZ, Li ZB, Zhang HX (2015) Microstructure and mechanical properties of Mg/Al bimetallic composite fabricated by compound casting. Mater Res Innov 19:S73–S78. https://doi.org/10.1179/1432891715Z.0000000001520

27. Jiang ZL, Fan ZT, Jiang WM, Li GY, Wu Y, Guan F (2018) Interfacial microstructures and mechanical properties of Mg/Al

bimetal produced by a novel liquid-liquid compound casting process. J Mater Process Technol 261:149–158. https://doi.org/10.1016/j.jmatprotec.2018.06.013

28. Li XB, Xiong SM, Guo ZP (2016) Characterization of the grain structures in vacuum-assist high-pressure die casting AM60B alloy. Acta Metall Sin (Engl Lett) 29(7):619–628. https://doi.org/10.1007/s40195-016-0430-1

29. Li XB, Xiong SM, Guo ZP (2016) Correlation between porosity and fracture mechanism in high pressure die casting of AM60B alloy. J Mater Sci Technol 32(1):54–61. https://doi.org/10.1016/j.jmst.2015.10.002

30. Yu WB, Ma CS, Ma YH, Xiong SM (2021) Correlation of 3D defect-band morphologies and mechanical properties in high pressure die casting magnesium alloy. J Mater Process Technol 288:116853. https://doi.org/10.1016/j.jmatprotec.2020.116853

31. Su CY, Li DJ, Wang J, Shi RH, Luo AA, Zeng XQ (2020) Enhanced ductility in high-pressure die casting Mg-4Ce-xAl-0.5Mn alloys via modifying second phase. Mater Sci Eng A 773:138870. https://doi.org/10.1016/j.msea.2019.138870

32. Margetis D (2009) Homogenization of reconstructed crystal surfaces: Fick's law of diffusion. Phys Rev E 79(5):052601. https://doi.org/10.1103/PhysRevE.79.052601

33. Ding HP, Bao XQ, Jamili-Shirvan Z, Jin JS, Deng L, Yao KF, Gong P, Wang XY (2021) Enhancing strength-ductility synergy in an ex situ Zr-based metallic glass composite via nanocrystal formation within high-entropy alloy particles. Mater Des 210:110108. https://doi.org/10.1016/j.matdes.2021.110108